DOT/FAA/TC-25/10

Federal Aviation Administration
William J. Hughes Technical Center
Aviation Research Division
Atlantic City International Airport
New Jersey 08405

Measuring the Fire Hazard of Aircraft Products in the Cone Calorimeter

August 2026

Final report

U.S. Department of Transportation
Federal Aviation Administration

Technical Report Documentation Page

Form DOT F 1700.7 (8-72) Reproduction of completed page authorized

1. Report No.	2. Government Accession No.	3. Recipient's Catalog No.
DOT/FAA/TC-25/10		

4. Title and Subtitle	5. Report Date
Measuring the Fire Hazard of Aircraft Products in the Cone Calorimeter	October 2025
	6. Performing Organization Code
7. Author(s) Richard E. Lyon, Tina Emami, Richard N. Walters and Timothy Salter	8. Performing Organization Report No.
9. Performing Organization Name and Address Fire Safety Branch Aviation Research Division Federal Aviation Administration Atlantic City International Airport, NJ 08405	10. Work Unit No. (TRAIS) 11. Contract or Grant No.
12. Sponsoring Agency Name and Address Obtain this information from your research-execution plan or similar plan.	13. Type of Report and Period Covered 14. Sponsoring Agency Code

15. Supplementary Notes

16. Abstract

A dimensionless group of reaction-to-fire properties called the product fire hazard Π is measured in one or more cone calorimeter experiments and describes the contribution of a combustible product-to-fire growth of materials used in buildings, construction, and passenger aircraft cabins. The product fire hazard Π is a sole explanatory variable for the fire performance of combustible solids in regulatory fire tests.

17. Key Words	18. Distribution Statement
cone calorimeter, combustibility, ignitability, heat release, ISO 5660, ISO 9705, ASTM E84, 14 CFR 25, flashover, fire growth	This document is available to the U.S. public through the National Technical Information Service (NTIS), Springfield, Virginia 22161. This document is also available from the Federal Aviation Administration William J. Hughes Technical Center at actlibrary.tc.faa.gov.

19. Security Classif. (of this report)	20. Security Classif. (of this page)	21. No. of Pages	22. Price
Unclassified	Unclassified	38	

Acknowledgements

The authors thank Prof. James G. Quintiere for guidance, insight and helpful discussions, and Dr. Marc Janssens for sharing valuable data.

Contents

Figures

Tables

Acronyms

Acronym	Definition
AEP	Available energy parameter
BCA	Building Code of Australia
BSL	Building Standards Law
CHF	Critical heat flux (for piloted ignition)
EHF	External heat flux
EU	European Union
FAA	Federal Aviation Administration
FSI	Flame spread index
HRP	Heat release parameter
HRR	Heat release rate
IBC	International Building Code
NFO	No flashover
PHRR	Peak heat release rate
t_{FO}	Time to flashover
THR	Total heat release
TRP	Thermal response parameter
TTI	Time to ignition

Executive summary

A dimensionless group of reaction-to-fire parameters called the product fire hazard Π is measured in one or more cone calorimeter experiments and describes the contribution of a combustible product-to-fire growth of materials used in buildings, construction, and passenger aircraft cabins. The product fire hazard Π is a sole explanatory variable for the fire performance of combustible solids in regulatory fire tests.

1 Background

Recent reviews of the classification of material fire safety describe how fire tests and regulations governing fire growth in compartments have evolved with the definition of what non-combustibility means (Sadaoui A, 2024; Ostman & Janssens, 2022; Babrauskas, 2017). Babrauskas (2017), Cleary and Quintiere (1991) and Tewarson (Tewarson, 1994) have argued that since heat release rate (HRR) is the primary variable driving fire growth, some combination of engineering variables that govern HRR at bench scale should replace the concept of noncombustibility at full-scale for regulatory purposes. A prior publication (Lyon, Measuring the Fire Growth Potential of Combustible Solids Using a Cone Calorimeter, 2024) describes combustibility as complementary to ignitability in the coupled and continuous process of ignition and burning that is fire growth:

$$\lambda = \ Combustibility \cdot Ignitability \equiv \left(\frac{\Delta h_c}{\Delta h_g}\right)\left(\frac{1}{E_{ign}}\right) = \ \frac{HRP}{E_{ign}} \tag{1}$$

In Equation 1, λ(m^2/J) is the fire growth potential, Δh_c(J/kg) is the specific enthalpy of flaming combustion, Δh_g(J/kg) is the specific enthalpy of fuel gasification, and HRP = $\Delta h_c/\Delta h_g$ is the combustibility ratio (Rasbash, 1976) or *heat release parameter* (Tewarson, 1994). The ignition energy, E_{ign} (J/m^2) is the thermal energy that has entered the solid from the fire at the time of ignition, t_{ign}, and can be expressed as the square of the *thermal response parameter* (see Table 1), TRP (Ws$^{1/2}$/m^2) (Tewarson, 1994), divided by the heat flux incident on the material surface from a fire or heater, $\dot{q}''_{ext}$:

$$E_{ign} \equiv \dot{q}''_{ext} t_{ign} = \dot{q}''_{ext} \left(\frac{\kappa\rho c_P \Delta T_{ign}^2}{\dot{q}''^{\,2}_{ext}}\right) = \ \frac{TRP^2}{\dot{q}''_{ext}} \tag{2}$$

In Equation 2, κ, ρ, and c_P are the thermal conductivity, density, and heat capacity of the solid, respectively; $\kappa\rho c_P$ is the thermal inertia; and $\Delta T_{ign} = T_{ign}$-T_0 is the difference between the piloted ignition and ambient temperatures. If the net heat flux entering the solid during ignition and burning is the difference between the heat flux entering the solid from an external heater or fire $\dot{q}''_{ext}$ and the surface flame $\dot{q}''_{flame}$, and the heat lost from the surface by reradiation to the environment, conduction into the solid and pyrolysis of the fuel during steady burning, $\dot{q}''_{loss}$, the fire growth potential of a combustible solid after ignition when $\dot{q}''_{flame} \approx \dot{q}''_{loss}$ can be written (Lyon, Measuring the Fire Growth Potential of Combustible Solids Using a Cone Calorimeter, 2024):

$$\lambda = \frac{HRP}{TRP^2}\, \dot{q}''_{net} = \frac{HRP}{TRP^2} \left(\dot{q}''_{ext} + \dot{q}''_{flame} - \dot{q}''_{loss}\right) = K\dot{q}''_{burn} \tag{3}$$

Equation 3 is a constitutive equation for the fire response of a combustible solid, λ to a thermal stress, $\dot{q}''_{net}$ for a combustible solid having fire compliance, K = HRP/TRP^2. After the solid ignites and burning commences, $\dot{q}''_{flame} \approx \dot{q}''_{loss} \approx$ 20-30 kW/m^2 and burning will be sustained if, $\dot{q}''_{ext} \approx \dot{q}''_{net} = \dot{q}''_{burn} \geq \lambda/K \approx$ 50 kW/m^2 (Lyon, Measuring the Fire Growth Potential of Combustible Solids Using a Cone Calorimeter, 2024; Lyon & Quintiere, Criteria for Piloted Ignition of Combustible Solids, 2007; Quintiere & Lian, 2009; Janssens, Carpenter, Huczek, Mehrafza, & Sauceda, 2006; Janssens, Carpenter, Huczek, Mehrafza, & Sauceda, Private communication; Tewarson, 1996).

The potential for fire growth is only realized as a fire hazard if the heat released by combustion of the fuel gases per unit area of burning surface is sufficient to grow the fire. If $\dot{Q}''(t)$ is the rate of heat release by flaming combustion of gaseous fuel per unit area of solid surface at time *t*, the total amount of heat that can be released by burning after the gaseous fuel is exhausted and flaming has ceased is

$$Q''_{total} = \int_0^{\infty} \dot{Q}''(t)dt \tag{4}$$

Acronyms for Q''_{total} measured in a cone calorimeter according to standard methods (ASTM International, 2023) (International Organization for Standardization, 2002) include the total heat release (THR) (Tewarson, 1994) and the available energy parameter (AEP) (Quintiere & Lian, 2009). The contribution of a combustible product to the growth of a fire can therefore be expressed in terms of the derived properties in Table 1 (Lyon, Measuring the Fire Growth Potential of Combustible Solids Using a Cone Calorimeter, 2024),

$$\Pi_p \equiv \lambda Q''_{total} = \frac{HRP \cdot Q''_{total}}{E_{ign}} = \frac{HRP \cdot Q''_{total}}{TRP^2/\dot{q}''_{ext}} \tag{5}$$

The rate of heat release by combustion during steady burning is $\dot{Q}''_{burn} = HRP \cdot \dot{q}''_{burn}$. The minimum (critical) heat release rate for upward burning and flame spread for a wide range of materials is $\dot{Q}''_{burn} = \dot{Q}''_{cr} \approx 70$ kW/m^2 (Lyon & Quintiere, 2007; Quintiere & Lian, 2009). Substituting, $\dot{q}''_{burn} = \dot{Q}''_{cr}/HRP \approx \dot{q}''_{ext}$ into Equation 5 gives an expression for the product fire hazard in terms of the minimum heat release rate for upward flame spread:

$$\Pi_b = \frac{Q''_{total}}{TRP^2/\dot{Q}''_{cr}} \tag{6}$$

An expression for Π that is amenable to calculation from the large amount of published $\dot{Q}'', \dot{q}''_{ext}, Q''_{total}$ cone calorimeter data for materials obtained under standard conditions (ASTM International, 2023; International Organization for Standardization, 2002) follows from a single-point approximation of the ignition energy, $E_{ign} \equiv \dot{q}''_{net} t_{ign} \approx \dot{q}''_{ext} t_{ign}$, and a single-point approximation of the heat release parameter (Lyon RE C. S., 2021), $HRP = \Delta\dot{Q}''/\Delta\dot{q}''_{ext} = \left(\dot{Q}''/\dot{q}''_{ext}\right)_{max} \approx \dot{Q}''_{max}/\dot{q}''_{ext}$:

$$\Pi = \lambda Q''_{total} \equiv \left(\frac{HRP}{E_{ign}}\right) Q''_{total} \approx \left(\frac{\dot{Q}''_{max}/\dot{q}''_{ext}}{\dot{q}''_{ext}\, t_{ign}}\right) Q''_{total} = \frac{\dot{Q}''_{max}/t_{ign}}{\dot{q}''^{2}_{ext}/Q''_{total}} \tag{7}$$

Equations 5-7 show that the contribution of a burning product to the growth of a fire Π can be evaluated using derived properties (Equation 5, Equation 6) or parameters measured in a single test (Equation 7) of forced flaming combustion in a cone calorimeter (Table 1).

Table 1. Quantities measured in the cone calorimeter used to compute Π

	Cone Calorimeter Quantities	**Notation**	**Acronym**	**Units**
Test Parameters	External Heat Flux (Irradiance)	$\dot{q}''_{ext}$	EHF	W/m^2
	Time to Sustained Piloted Ignition	t_{ign}	TTI	Seconds
	Heat Release Rate	$\dot{Q}''$	HRR	W/m^2
	Maximum (Peak) Heat Release Rate	$\dot{Q}''_{max}$	PHRR	W/m^2

	Cone Calorimeter Quantities	Notation	Acronym	Units
	Total Heat Released by Combustion	Q''_{total}	THR	J/m^2
Derived Fire Properties	Heat Release Parameter	$\Delta\dot{Q}''/\Delta\dot{q}''_{ext}$	HRP	(–)
	Thermal Response Parameter	$\Delta\dot{q}''_{ext}/\Delta t_{ign}^{-1/2}$	TRP	Ws$^{1/2}$/m^2
	Critical Heat Flux for Piloted Ignition	$\dot{q}''_{ign}$	CHF	W/m^2

2 Approach

The resistance of a product to burning in a particular fire test is assumed to depend only on Π and the intensity of the thermal insult to the product in the test $\dot{q}''_{ext}$. For example, in the room corner fire test ISO 9705 (International Organization for Standardization, 2016) burning resistance *F* will be measured as the time to flashover, while *F* will be the reciprocal of the flame spread index in the Steiner Tunnel test ASTM E84 (ASTM International, 2023). Burning resistance *F* in a full-scale aircraft cabin is defined as the fraction of bench-scale fire tests that satisfy the flammability requirements for materials of construction, 14 CFR Part 25 Appendix F (Federal Aviation Administration, 2004; Federal Aviation Administration, 2000). If Π and $\dot{q}''_{ext}$ are only variables responsible for a product's burning resistance in a particular test, $F(\dot{q}''_{ext}, \Pi)$, and the total differential for the product's burning resistance is

$$dF = \left(\frac{\partial F}{\partial \dot{q}''_{ext}}\right)_{\Pi} d\dot{q}''_{ext} + \left(\frac{\partial F}{\partial \Pi}\right)_{\dot{q}''_{ext}} d\Pi \tag{8}$$

At a particular value of *F*,

$$\left(\frac{dF}{d\dot{q}''_{ext}}\right)_{F} = 0 = \left(\frac{\partial F}{\partial \dot{q}''_{ext}}\right)_{\Pi} + \left(\frac{\partial F}{\partial \Pi}\right)_{\dot{q}''_{ext}} \left(\frac{d\Pi}{d\dot{q}''_{ext}}\right)_{F} \tag{9}$$

Rearranging Equation 9 with $(d\Pi/d\dot{q}''_{ext})_F = Q''_{total}HRP/TRP^2 = \Pi/\dot{q}''_{ext}$ as per Equation 5,

$$-\left(\frac{\partial F}{\partial \Pi}\right)_{\dot{q}''_{ext}} = \frac{(\partial F/\partial \dot{q}''_{ext})_{\Pi}}{(d\Pi/d\dot{q}''_{ext})_{F}} = \frac{(\partial F/\partial \dot{q}''_{ext})_{\Pi}}{Q''_{total}HRP/TRP^2} = \frac{(\partial F/\partial \ln[\dot{q}''_{ext}])_{\Pi}}{\Pi} \equiv \frac{c_1}{\Pi^n} \tag{10}$$

The general solution to Equation 10 is:

$$F = \frac{F_0}{\Pi^b} + c_2 \tag{11}$$

The constants are $F_0 = c_1/b = F(\Pi = 1)$ and $b = (1+n)$. The asymptotic limits, $-(\partial F_R/\partial \Pi)_{\dot{q}''_{ext}} = 0, \infty$ at $\Pi = \infty, 0$, require that $c_2 = 0$ for all positive values of b, so

$$F = \frac{F_0}{\Pi^b} \tag{12}$$

Equation 12 states that the burning resistance of a product *F* decreases exponentially with product fire hazard Π. This power law relationship between *F* and Π is scale invariant, because for any multiplication factor *C*, the shape of *F versus* Π does not change with rescaling because $F(C) = F_0/(C\Pi)^b = (F_0/\Pi^b)/C^b = F(\Pi)G(C)$. Equation 12 is predicated on the hypothesis that Π is the sole explanatory variable for the fire performance of a product in forced flaming combustion and that b, F_0 characterize the thermal insult to the product $\dot{q}''_{ext}(F_0, b)$ in the fire test.

Equation 12 shows *F* to be a monotonically decreasing function of Π without a discontinuity or an inflection point that could be interpreted as a critical value or threshold. However, a characteristic feature of *F* is an abrupt change in slope at or "knee" in the power law curve. The tangent to the curve of *F versus* Π at maximum curvature is the ratio of the experimental range to the experimental domain of *F*, both referenced to the origin:

$$-\left(\frac{dF}{d\Pi}\right)_{threshold} = \frac{bF_0}{\Pi^{1+b}} \equiv \frac{Range\ of\ F}{Domain\ of\ F} = \frac{F_{max}}{\Pi_{max}} \tag{13}$$

The product fire hazard at the point of maximum curvature is therefore

$$\Pi^* = \left[\frac{b\Pi_{max}}{F_{max}/F_0}\right]^{1/(1+b)} \tag{14}$$

Equation 14 can be interpreted as the fire safety threshold for products in a particular fire test. The corresponding product fire resistance F^* is proportional to Π^* for a particular fire test (b, F_{max}) and selection of products (Π_{max}) and is obtained from Equation 12 and Equation. 14 as

$$F^* = \frac{F_0}{\Pi^*} = \frac{F_{max}/\Pi_{max}}{b} \cdot \Pi^* = C(b) \cdot \Pi^* \quad (15)$$

A recent publication showed that Π successfully ranks the intrinsic fire hazard of materials as well as correlating fire growth of isolated products and those attached to the ceilings and walls of compartments (Lyon, Measuring the Fire Growth Potential of Combustible Solids Using a Cone Calorimeter, 2024). In this publication, Π is shown to be the sole explanatory variable for the burning resistance of products in forced flaming combustion, such as the full-scale room corner fire test ISO 9705 (International Organization for Standardization, 2016), the Steiner Tunnel Test ASTM E84 (ASTM International, 2023), and post-crash fire tests of aircraft cabin materials (Federal Aviation Administration, 2004; Federal Aviation Administration, 2000). Finally, Π is shown to provide a consistent ranking of the fire test performance of products across international building codes (Ostman & Janssens, 2022; Janssens, Carpenter, Huczek, Mehrafza, & Sauceda, 2006).

3 Experimental

3.1 Methods

Heat release rate histories of commercial materials were measured in the Fire Test Laboratory at the Federal Aviation Administration (FAA) Technical Center using a cone calorimeter manufactured by Fire Testing Technology, East Grinstead, UK, and operating on the oxygen consumption principle according to ASTM E 1354 (ASTM International, 2023). Figure 1 shows a test being conducted in the FAA cone calorimeter using a sample holder with the edge frame and wire grid, insulated rear sample face, and electric spark igniter that were used for all tests at the recommended 25-mm separation between the conical heater and the sample surface. Cone calorimeter tests were conducted in triplicate on 10 cm x 10 cm square samples ranging in thickness from 3 mm to 25 mm. Heat release rate histories from the literature were measured (Quintiere & Lian, 2009; Janssens, Carpenter, Huczek, Mehrafza, & Sauceda, 2006; Janssens, Carpenter, Huczek, Mehrafza, & Sauceda, Private communication; Ostman & Tsantaridis, 1995;

Ostman & Tsantaridis, 1994; Lyon & Safronava, 2013) for products of various thickness using contemporary versions of cone calorimeter standards (ASTM International, 2023; International Organization for Standardization, 2002) to obtain the test parameters and derived properties listed in Table 1 for calculation of Π. The uncertainty of Equation 7 for Π is 44% at 95% confidence, estimated from a propagation of error analysis using the reproducibility standard deviation at the geometric mean of the range reported in the precision and bias statement of ASTM E1354-23 (ASTM International, 2023) for t_{ign}, $\dot{Q}''_{max}$ and Q''_{total}.

Full-scale ISO 9705 room corner fire tests (International Organization for Standardization, 2016) of wall linings, wood, and other construction products were conducted by Janssens et. al. (2006) or collected by Ostman and Tsantaridis (Ostman & Tsantaridis, 1995; Ostman & Tsantaridis, 1994) and Quintiere and Lian (2009). An ISO 9705 test of wall lining materials at 0 and 10:30 minutes into the test are shown in Figure 2. Janssens et al (2006) also conducted measurements of the ISO 9705 construction products in the Steiner Tunnel test (ASTM E84) shown in Figure 3.

Figure 1. Conducting a test in the cone calorimeter

Figure 2. Room corner fire test (ISO 9705) at 0 and 10:38 minutes

Figure 3. Steiner Tunnel test apparatus (ASTM E84)

The goal of all these studies was to correlate the fire performance of construction products and interior lining materials at full scale with the fire test parameters and derived properties in Table 1 measured under controlled conditions at bench-scale to establish an engineering basis for full-scale results, reduce the cost of product development, or establish classification schemes for materials in regulatory standards.

Flammability tests of lightweight polymeric materials were conducted in the Fire Test Laboratory at the FAA Technical Center according to 14 CFR 25 Part 25 Appendix F standard procedures (Federal Aviation Administration, 2004; Federal Aviation Administration, 2000). The metrics for these tests of piloted ignition and burning of solid materials include upward flame spread on a vertical specimen after 12-second ignition with a small (Bunsen burner) flame, the sensible HRR of large area cabin materials in a vertical orientation using the thermopile method at $\dot{q}''_{ext}$ = 35 kW/m^2, and a radiant panel test for horizontal burning of thermal-acoustic insulation in a heat flux gradient.

3.2 Materials

Wood, plastic, paper, and composite products whose test results were reported in the literature (Quintiere & Lian, 2009; Janssens, Carpenter, Huczek, Mehrafza, & Sauceda, 2006; Janssens, Carpenter, Huczek, Mehrafza, & Sauceda, Private communication; Ostman & Tsantaridis, 1995; Ostman & Tsantaridis, 1994; Lyon & Safronava, A Probabilistic Analysis of Pass/Fail Fire Tests, Final Report DOT/FAA/TC-12/13, 2013) ranged in thickness from 3 mm to 38 mm. Room lining materials having thickness < 1 mm were adhered to 13-mm thick Type X gypsum board (sheetrock/drywall) for testing at bench- and full-scale. Plastics that were tested at FAA to 14 CFR 25 Appendix F had a wide range of flammability, representative of those used in aircraft interiors, and were obtained from commercial sources with thickness of 0.1-0.3 cm. High purity (>99%) gases from local suppliers were used for all FAA fire tests.

4 Results

4.1 Product Hazard (Π)

The fire test parameters in Table 1 were measured in triplicate by Janssens et. al. (Private communication) for each product in Table 2 using the cone calorimeter according to ASTM E1354 (2023) at external heat fluxes, $\dot{q}''_{ext}$ = 25, 50, 75 and 100 kW/m^2. Some products did not ignite and burn at $\dot{q}''_{ext}$ = 25 kW/m^2 in the cone calorimeter, but all products ignited and burned at $\dot{q}''_{ext} \geq 50$ kW/m^2. The derived fire properties HRP, TRP of Table 1 were computed from

Janssen's data (Private communication) for use in this paper as the slopes $\Delta\dot{Q}''_{max}/\Delta\dot{q}''_{ext}$ and $\Delta t_{ign}^{-1}/\Delta\dot{q}''_{ext}$ of the linear least squares regression lines of $\dot{Q}''_{max}$ or $t_{ign}^{-1/2}$ on $\dot{q}''_{ext}$, respectively.

Mean values of Π for each product in Table 2 at $\dot{q}''_{ext}$ = 25, 50, 75 and 100 kW/m^2 were computed using Equation 7 and are plotted in Figure 4, which shows that Π for each product at $\dot{q}''_{ext}$ = 50 kW/m^2 is within one standard deviation of the mean Π for that product at all $\dot{q}''_{ext}$ and within the uncertainty of the calculation of Π by propagation of error (± 44%) in most cases.

Figure 5 is a plot of Π for Janssens' data (Private communication) at $\dot{q}''_{ext}$= 50 kW/m^2 using the fire test parameters $\dot{Q}''_{max}, t_{ign}$ and Q''_{total} from Table 1 in Equation 7 versus Π for the same product at $\dot{q}''_{ext}$= 50 kW/m^2 computed using the derived fire properties HRP, TRP, and Q''_{total} from Table 1 in Equation 5. Figure 5 shows that Π computed from the fire parameters in a single test at $\dot{q}''_{ext}$ = 50 kW/m^2 by Equation 7 displayed on the ordinate is, in most cases, within the uncertainty (44%) of Π_p computed from the derived properties obtained from multiple $\dot{q}''_{ext}$ by Equation 5 on the abscissa.

Figure 6 is a plot of the product fire hazard Π_p calculated from Quintiere and Lian's (2009) HRP, TRP, and Q''_{total} in Equation 5 with $\dot{q}''_{ext}$ = 50 kW/m^2 versus Π_b of Equation 6 with THR, TRP, and $\dot{Q}''_{cr}$ = 70 kW/m^2 (Lyon & Quintiere, 2007; Quintiere & Lian, 2009). Qualitative agreement between these expressions for Π using derived properties at constant heat flux (Equation 5) and constant (critical) heat release rate (Equation 6) is observed with a correlation coefficient (R = 0.79).

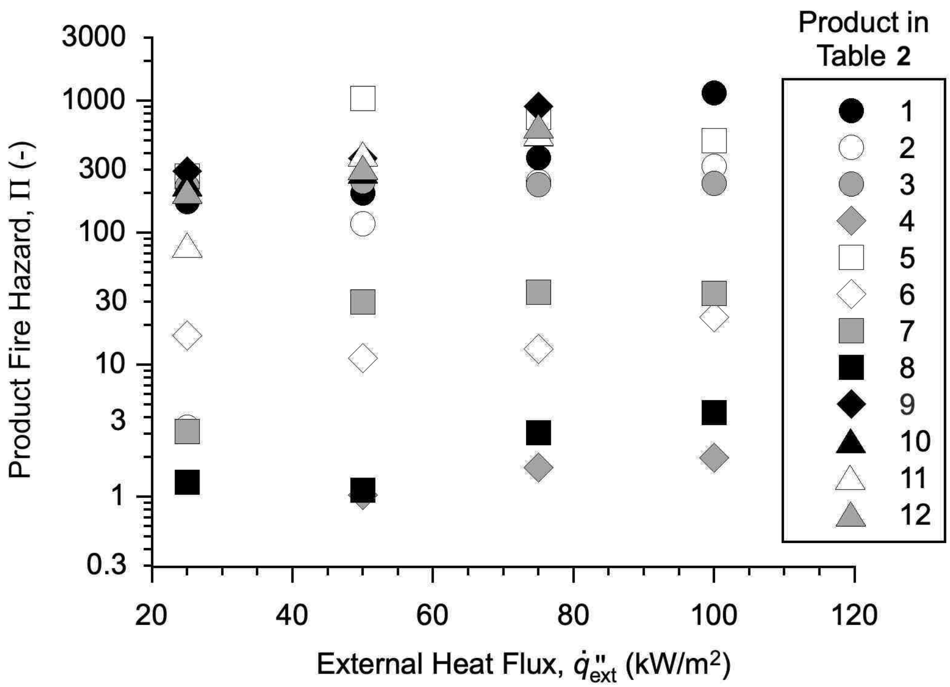

Figure 4. Fire hazard of the products in Table 2 computed at $\dot{q}''_{ext}$ = 25, 50, 75 and 100 kW/m^2 from data from Janssens

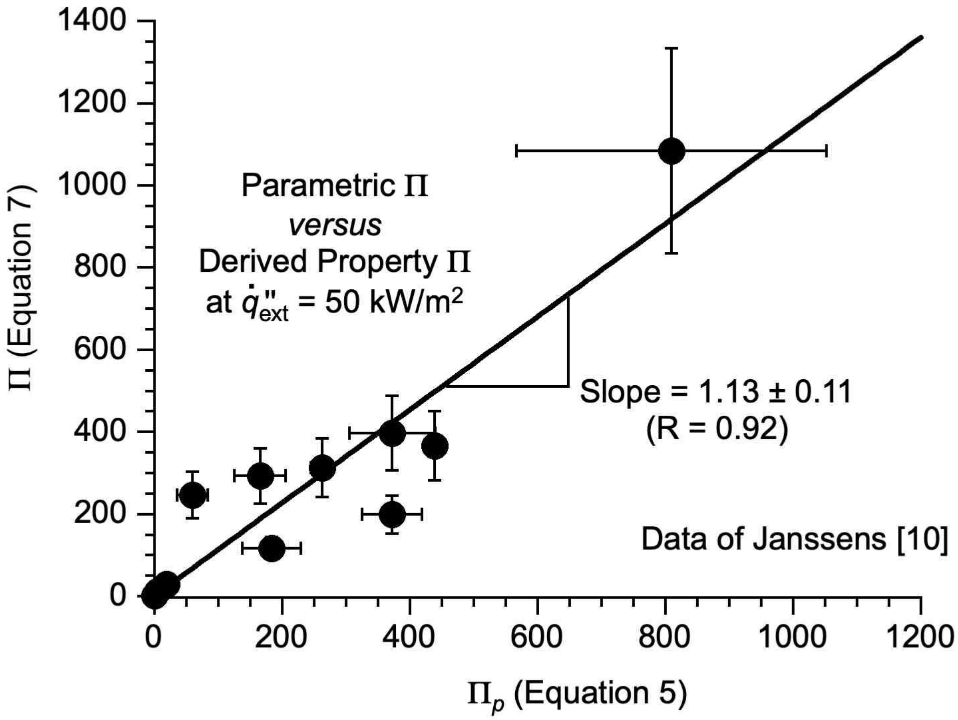

Figure 5. Product fire hazard Π from the fire test parameters (Equation. 7) versus derived properties (Equation. 5) in Table 1 at $\dot{q}''_{ext}$ = 50 kW/m^2

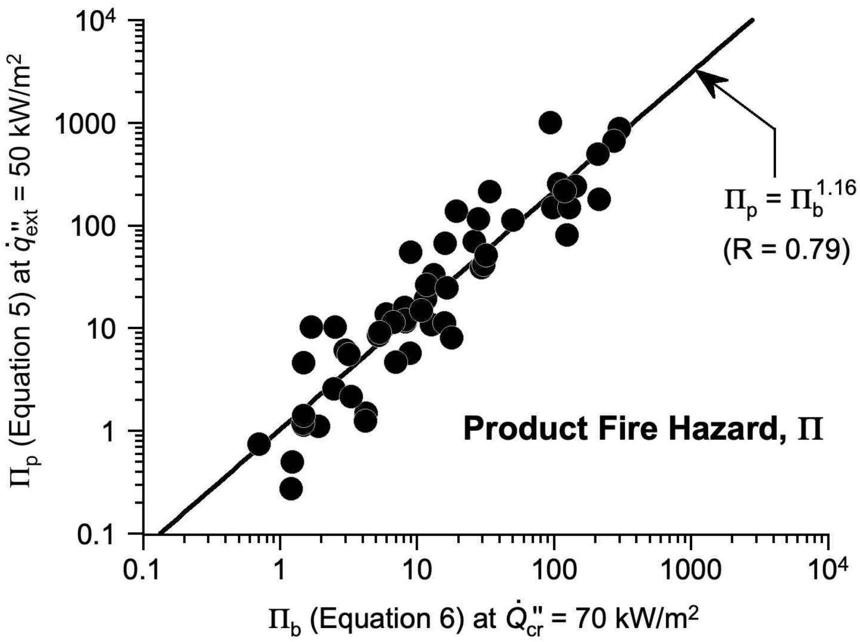

Figure 6. Single heat flux versus single (critical) HRR calculation of Π

4.2 Room corner fire test (ISO 9705)

Janssens et. al. (2006) measured cone calorimeter test parameters for the 12 construction products in Table 2 as well as the flame spread index (FSI) in the Steiner Tunnel test ASTM E84 (ASTM International, 2023), and the time to reach a 1 MW fire (flashover) in the ISO 9705 room corner fire test (International Organization for Standardization, 2016). Also in that report were the International Building Code (IBC) classification of the test results for 9 of the 12 products in Table 2 attached to the walls and ceiling of the ISO 9705 room corner fire test. Products that did not flashover in the two-stage 100 kW/10 min + 300 kW/10 min test are marked as no flashover (NFO).

Table 2. Time to flashover (t_{FO}), Flame Spread Index (FSI), IBC classification, and Π for construction products

ID	Product	Π	t_{FO} (min)	FSI	IBC Class
1	Polyisocyanurate Foam	1084 ± 243	0.25 ± 0.09	54 ± 8	B
2	White Pine Planks	397 ± 67	—	92 ± 4	C
3	Oriented Strand Board 1	366 ± 14	—	139 ± 8	C
4	White Oak Planks	313 ± 17	—	81 ± 5	C
5	Oriented Strand Board 2	293 ± 40	2.25	151 ± 17	C
6	Glass Fiber Reinforced Plastic	246 ± 24	2.23	130 ± 6	C
7	Douglas Fir Plywood	199 ± 47	2.75 ± 0.11	111 ± 6	C
8	FRT Douglas Fir Plywood	117 ± 46	10.63 ± 0.07	14 ± 2	A
9	Textile Wall Covering*	29 ± 3	NFO	20 ± 5	A
10	Vinyl Wall Covering*	11 ± 1	10.67 ± 0.16	28 ± 0	B
11	Type X Gypsum Board	1 ± 0	NFO	5 ± 0	A
12	Paper Wall Covering*	1 ± 0	NFO	10 ± 1	A
	Test Method	**ASTM E1354**	**ISO 9705**	**ASTM E84**	

*Adhered to Type X Gypsum Board.

Ostman and Tsandaridis (Ostman & Tsantaridis, 1995; Ostman & Tsantaridis, 1994) compiled cone calorimeter data from the literature for $\dot{Q}''_{max}$, Q''_{total} and t_{ign} at $\dot{q}''_{ext}$= 50 kW/m^2 for 27 wall linings and construction materials. These fire test parameters of Table 1 were used to calculate the Π values in Table 3 (Federal Aviation Administration, 2004; Federal Aviation Administration, 2000) using Equation 7. Two fire retardant wood products out of 27 wood products (7%) did not ignite at $\dot{q}''_{ext}$ = 50 kW/m^2 in the cone calorimeter. All of these materials were tested in ISO 9705 for the time to reach a 1 MW fire (t_{FO}) for the 27 materials in Table 3 mounted on the walls and ceiling of the room corner fire test (International Organization for Standardization, 2016). Products that did not flashover in the two-stage ignition, 20-min test are marked as NFO. Ostman and Tsandaridis (Ostman & Tsantaridis, 1994) performed a linear regression of the duplicate times to flashover, t_{FO} in ISO 9705 on t_{ign} and Q''_{total} measured in the cone calorimeter at $\dot{q}''_{ext}$ = 50 kW/m^2 with R = 0.90, but found a higher correlation (R = 0.97) when the product density, ρ(kg/m^3), was included to account for the thermal inertia that is explicit in TRP of Π:

$$t_{FO}(min) = 1 + \frac{0.07}{60}\frac{t_{ign}^{0.25}\rho^{1.7}}{Q''^{\,1.3}_{total}} \tag{16}$$

Table 3. ISO 9705 times to flashover and Π for wood products

Product	**Π**	**Thickness (mm)**	**Measured t_{FO} (min)**	**Eqn. 16 t_{FO} (min)**
Medium Density Wood Fiberboard	400	9	2.18	3.08
Ordinary Birch Plywood	332	12	2.50	2.43
Particle Board	314	22	—	2.73
Birch Plywood	279	12	2.28	2.55
Hardboard	266	6	—	3.42
Insulating Wood Fiberboard	229	13	—	1.30
Particle Board	224	10	2.62	2.40
Particle Board	210	12	—	2.90
Insulating Wood Fiberboard	198	13	—	1.27
Beech Plywood	187	15	—	3.92
Wood Panel, Spruce	139	11	2.18	2.37
Medium Density Wood Fiberboard	138	12	1.00	3.08
FR Insulating Wood Fiber Board	137	15	—	1.85
FR Beech Plywood	111	15	—	5.05

Product	Π	Thickness (mm)	Measured t_{FO} (min)	Eqn. 16 t_{FO} (min)
FR Medium Density Wood Fiberboard	111	9	—	12.5
FR Particle Board, Type B1	71	16	10.5	8.90
Beech Plywood	69	5	—	2.05
FR Particle Board	58	22	—	6.72
FR Particle Board, Pyroex	57	13	—	6.43
FR Hardboard	34	6	—	10.3
FR Particle Board	9.7	22	—	11.6
FR Medium Density Wood Fiberboard	4.9	12	—	9.52
FR Particle Board	0.57	12	NFO	14.6
FR Plywood, Noncom	0.40	13	—	14.9
FR Plywood, Injecta	0.14	9	NFO	22.2
FR Particle Board, Firex	NI	12	—	20.0
FR Beech Plywood	NI	15	—	20.0

Quintiere and Lian (Quintiere & Lian, 2009) analyzed cone calorimeter test data and ISO 9705 room corner test results for 54 room lining materials from several sources and computed HRP, TRP, Q''_{total}, and the critical heat flux for ignition (CHF) from $\dot{Q}''(t)$ histories of these products. Cleary, Quintiere and Lian (Cleary & Quintiere, 1991) (Quintiere & Lian, 2009) modeled flashover in ISO 9705 as a discontinuity in the fire growth rate at the critical heat release rate for upward flame spread, $\dot{Q}''_{cr} \approx 100$ kW/m^2, using HRP, TRP, Q''_{total} and CHF of Table 1 and the net heat flux in the environment, $\dot{q}''_{net} = \dot{q}''_{ext} - CHF \approx 60$ kW/m^2. Quintiere and Lian's (Quintiere & Lian, 2009) reported HRP, TRP, and Q''_{total} were used to calculate Π_b by Equation 6 at the critical heat release rate for sustained horizontal burning in the cone calorimeter $\dot{Q}''_{cr} = 70$ kW/m^2 (Lyon & Quintiere, 2007), and the results are given in Table 4. Products that did not flashover in the two-stage ignition, 20-min test are marked NFO. Quintiere et.al. (Cleary & Quintiere, 1991; Quintiere & Lian, 2009) found that flashover did not occur in the two-stage, 20-min, ISO 9705 test if

$$\left\{\frac{\dot{q}''_{net} \cdot HRP}{\dot{Q}''_{cr}} - \frac{HRP \cdot TRP^2}{\dot{q}''_{net} \cdot THR}\right\} - 1 \leq -1 \qquad (17)$$

Equation 6 can be factored out of Equation 17 to obtain Π of Quintiere's (Cleary & Quintiere, 1991; Quintiere & Lian, 2009) flashover criterion for ISO 9705 using the reported $\dot{Q}''_{cr} = 100\ kW/m^2$ and $\dot{q}''_{net} = \dot{q}''_{ext} - CHF = 60\ kW/m^2$:

$$\Pi \leq \left(\frac{\dot{Q}''_{cr}}{\dot{q}''_{net}}\right)^2 = \left(\frac{100\ kW/m^2}{60\ kW/m^2}\right)^2 = 2.78 \tag{18}$$

Figure 7 (International Organization for Standardization, 2016; Quintiere & Lian, 2009; Janssens, Carpenter, Huczek, Mehrafza, & Sauceda, 2006; Ostman & Tsantaridis, 1995; Ostman & Tsantaridis, 1994) is a plot of the times-to-flashover of the 95 products in Tables 2-4 tested on the walls and ceiling of the ISO 9705 room versus Π at $\dot{q}''_{ext}$ = 50 kW/m^2 (Equation 5 and Equation 7) or at $\dot{Q}''_{cr}$ = 70 kW/m^2 (Equation 6). Products that did not flashover in the 20-min test were assigned a flashover time of 25 minutes for this analysis, i.e., NFO ≡ 25 minutes in Tables 2-4. The solid line through all the data points in Figure 7 is Equation 12 with non-linear least-squares regression coefficients, F_0 = 27 min, and b = 0.46 having correlation coefficient R = 0.66.

Table 4. ISO 9705 t_{FO} and fire hazard (Π_b) of construction products lining the walls and ceiling of the room corner test

Π_b	t_{FO} (min)		Π_b	t_{FO} (min)		Π_b	t_{FO} (min)
297	0.100		19.3	1.33		5.30	NFO
272	0.683		17.7	5.70		5.21	11.2
211	10.5		16.5	NFO		4.21	NFO
209	0.983		15.9	NFO		4.19	NFO
142	2.18		15.8	5.10		3.29	NFO
129	2.37		13.2	10.2		3.15	NFO
123	1.78		12.7	1.25		2.97	NFO
119	2.62		11.7	13.9		2.50	NFO
108	2.18		11.5	3.58		2.46	NFO
96.8	0.900		10.6	10.8		1.90	NFO
93.4	2.35		8.94	10.6		1.68	NFO
49.8	1.70		8.79	11.2		1.49	NFO
33.7	0.717		8.19	10.7		1.48	NFO
31.7	7.75		8.15	2.38		1.47	NFO
30.3	2.67		8.10	10.5		1.46	NFO
29.4	1.92		6.95	167		1.22	NFO
27.8	1.60		6.66	11.2			
26.0	1.45		5.95	10.2			

The fire hazard threshold in the ISO 9705 test, $\Pi^* = 74$ at $F^* = 3.7$ min is shown as a red asterisk in Figure 7 computed from the regression coefficients and the experimental domain $\Pi_{max} = 1084$ and $F_{max} \equiv 25$ of Table 2 using Equation 14 and Equation 15, respectively. Although Equation 12 captures the overall trend in flashover times with product fire hazard, a single (deterministic) value of Π that precludes flashover is not observed in Figure 7, as indicated by the multiple values of Π at $F_{max} = 25$ min.

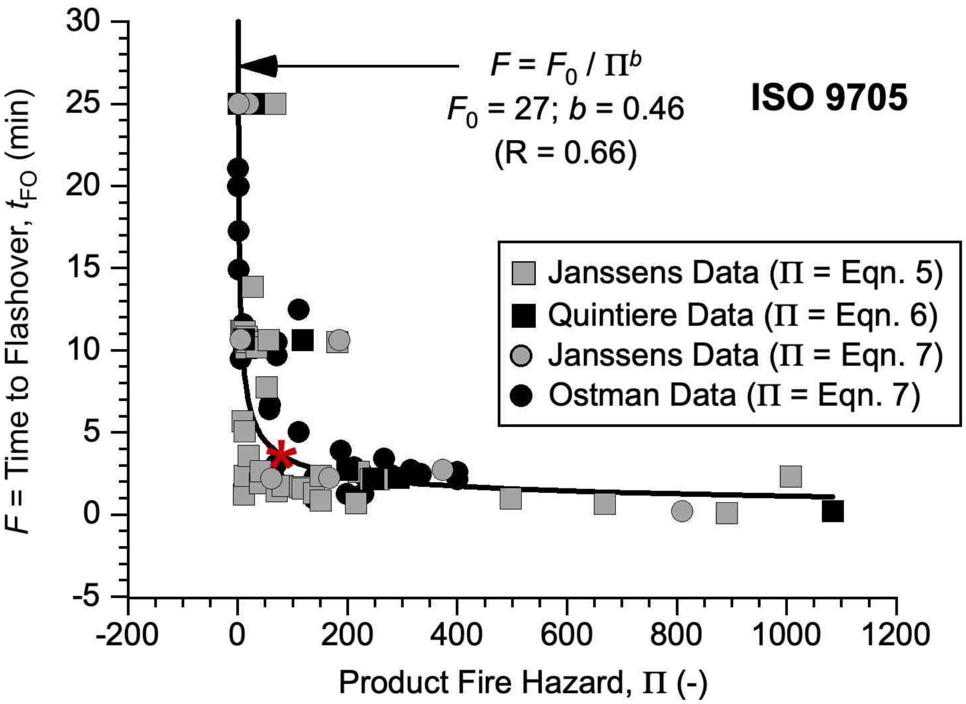

Figure 7. Time-to-flashover of 95 different products in the ISO 9705 room corner fire test versus Π

To account for the uncertainty in fire test results, a probabilistic analysis of ISO 9705 can be applied to the data in Figure 7 if Π is the sole explanatory variable for F and ISO 9705 is treated as a pass/fail test with a binary no-flashover/ flashover (0/1) outcome (Lyon & Safronava, 2013). Figure 8 shows the results of the probabilistic analysis using the phlogistic response function, $p = 1/[1+(\Pi_0/\Pi)^a]$ shown in the legend, for the likelihood of flashover. The cumulative probability p is regressed on the 151 binary data, yielding nonlinear least squares regression coefficients, Π_0 = 7.2 and a = 2.27. Consequently, a product with fire hazard Π = 7.2 has a 50% chance of flashover in the 20-min, two-stage ignition ISO 9705 room corner test, while a product satisfying Quintiere's flashover criterion, Π ≤ 2.78 (Equation 18) has less than a 10% chance of reaching flashover. These estimates of the product burning resistance versus Π are confirmed by inspection of Tables 2-4. The large overlap of the binary flashover data versus Π in Figure 8 below the fire hazard threshold Π* = 74 of Figure 7 reflects the combined uncertainties of Π (44%) and t_{FO} (58%) (Ostman & Tsantaridis, 1995). Consequently, only half ($R^2 = (0.72)^2$ = 52%) of the 151 data points are correlated by the phlogistic response function.

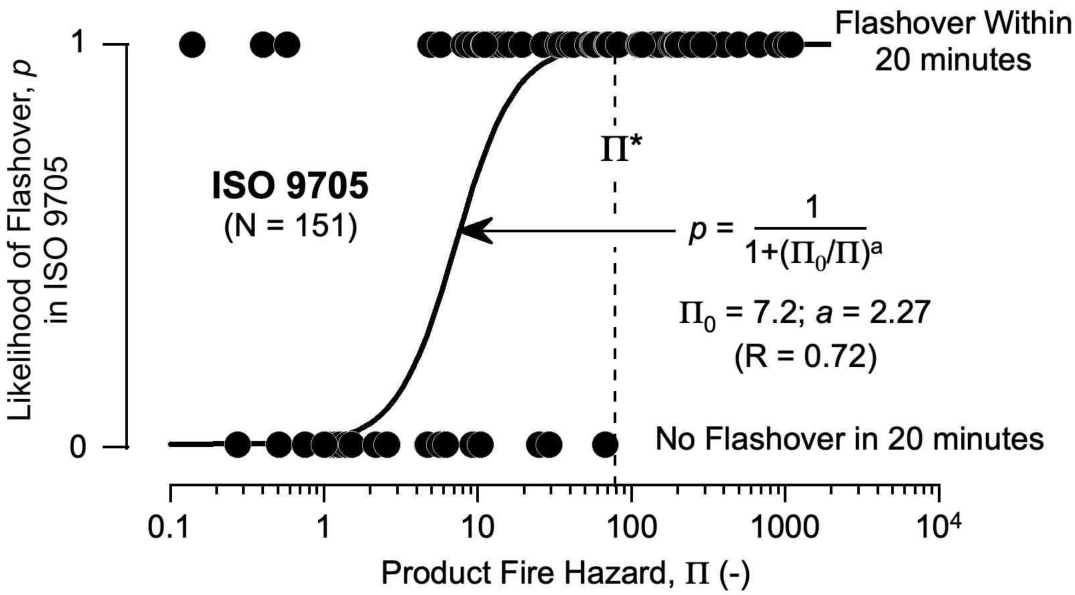

Figure 8. Probabilistic analysis of the data in Figure 7 for product flashover in ISO 9705

4.3 Steiner Tunnel test (ASTM E84)

Figure 9 is plot of the flame spread index FSI in the Steiner Tunnel test ASTM E84 (ASTM International, 2023) for the products in Table 2 (Janssens, Carpenter, Huczek, Mehrafza, & Sauceda, 2006), plotted as $F \equiv 100/\text{FSI}$ versus the corresponding product fire hazard Π using Equation 7 at $\dot{q}''_{ext}$ = 50 kW/m^2. Nonlinear least-squares regression of Equation 12 on the data in Figure 9 gives $F_0 = 15.8$ and $b = 0.41$, for the solid line through the data points. The abrupt change in the slope of F *versus* Π is observed in Figure 9 as a red asterisk at the fire hazard threshold, $\Pi^* = 64$ at $F^* = 2.87$ (FSI* = 35), computed using Equation 14 and Equation 15, respectively, at $\Pi_{max} = 1084$ and $F_{max} = 100/5 = 20$ of Table 2.

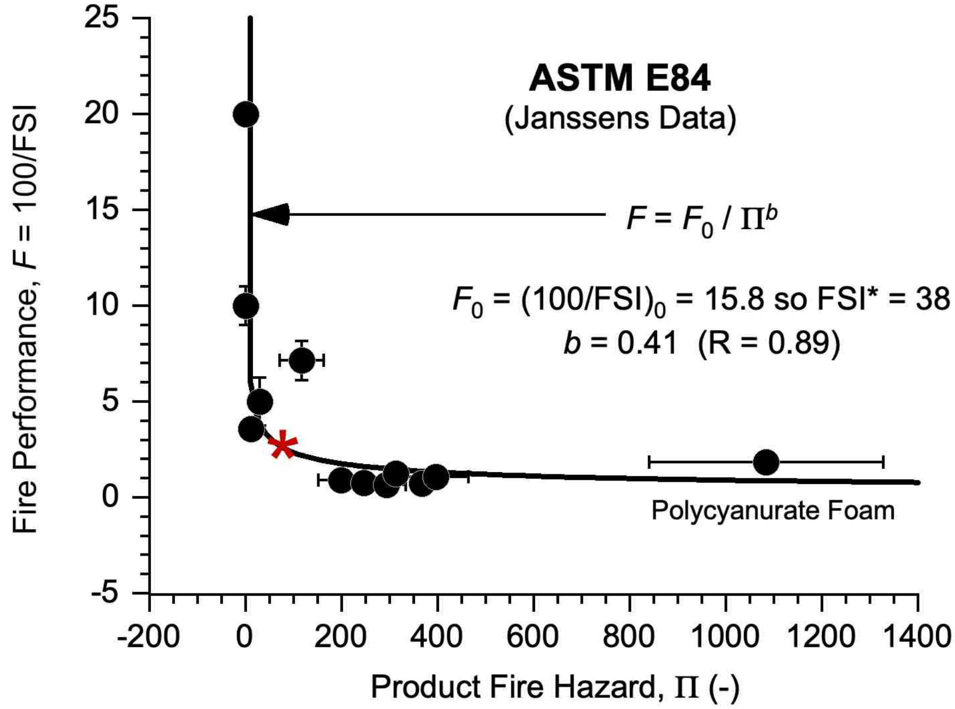

Figure 9. Fire performance of construction products, F Π 100/FSI in the Steiner Tunnel test (ASTM E84) versus Π

4.4 Federal airworthiness regulations (14 CFR 25)

The seven materials in Table 5 were tested for flammability in four bench-scale fire tests separately representing the ignitability, flame spread, and combustibility of materials used in passenger aircraft cabins (Hill, Brown, Speitel, Johnson, & Sarkos, 1984; Hill, Eklund, & Sarkos, 1985). These tests are described in the Fire Test Handbook (Federal Aviation Administration, 2000) of 14 CFR 25 Appendix F (Federal Aviation Administration, 2004). The metrics (i) in these tests include burn length, burning time, and time of flaming drops in the 12-second ignition vertical Bunsen burner test, the peak heat release rate and total heat release in the sensible heat release rate test for cabin materials, and the burn length and burning time in the horizontal radiant panel test for thermal-acoustic insulation. Each of these seven flammability metrics, i, received a value of 1 if it met the 14 CFR 25 criterion for cabin materials in that test, or a value of 0 if it did not. The fire hazard of each product in an aircraft cabin was defined as the fraction of the N_0 = 7 metrics meeting the 14 CFR 25 criterion for interior cabin materials, $F = \sum i/7 = N/N_0$ = FAR Score.

The products listed in Table 5 were also tested in the cone calorimeter according to ASTM E1354 (ASTM International, 2023) at an external heat flux, $\dot{q}''_{ext}$ = 50 kW/m^2. The average product fire hazard Π listed in the first column of Table 5 was calculated by Equation 7 from triplicate measurements of the fire test parameters in Table 1. Figure 10 is a plot of the burning resistance of the products in Table 5 in an aircraft cabin, $F = N/N_0$ *versus* Π. The solid line through the data points is the nonlinear least-squares regression line for Equation 12 with coefficients F_0 = 1.0, b = 0.22 over the domain Π_{max} = 800. Equation 14 and Equation 15 give the fire hazard threshold shown as a red asterisk in Figure 9, Π* = 67 at F^* = 0.40 for Π_{max} = 765, F_{max} = 1.00 of Table 6.

Table 5. Product fire hazard (Π) and FAA fire test performance (*F*)

Product	**Π (–)**	***N* / N₀**	***F***
Fiberglass Filled Polytetrafluoroethylene/PTFE	1 ± 0	7/7	1.00
Hexfluoropropylene/vinylidene fluoride copolymer	14 ± 1	4/7	0.57
Polyvinylchloride (transparent)	18 ± 2	5/7	0.71
Polyetherimide	22 ± 3	5/7	0.71
Carbon Fabric Reinforced Epoxy	110 ± 12	1/7	0.14
Glass Fabric Reinforced Phenolic	158 ± 17	3/7	0.43
Crosslinked Polystyrene	765 ± 97	0/7	0
Test Method	**ASTM E1354**	**14 CFR 25 Fire Test Handbook**	

A probabilistic analysis of the data in Table 5, plotted in Figure 10, can be performed as follows. If the likelihood flashover in an airplane fuselage within 4 minutes of a post-crash fuel fire (Hill, Brown, Speitel, Johnson, & Sarkos, 1984; Hill, Eklund, & Sarkos, Aircraft Interior Panel Test Criteria Derived from Full-Scale Fire Tests, 1985) is equated to the fraction of bench-scale tests that do not satisfy 14 CFR 25, then nonlinear least squares regression of $1\text{-}F = 1\text{-}N/N_0$ on the product fire hazard Π gives the solid line for the probabilistic response function $p = 1/\{1+[\Pi_0/\Pi]^a\}$ in Figure 11. Error bars for p are average standard deviation of 14 CFR 25 fire tests (±15%) (Safronava N, August 2022), while error bars for Π are the uncertainty (±22%) of its calculation from cone calorimeter test parameters in Table 1 based on the reproducibility of the parameter means in the ASTM E1354 precision and bias statement (ASTM International, 2023).

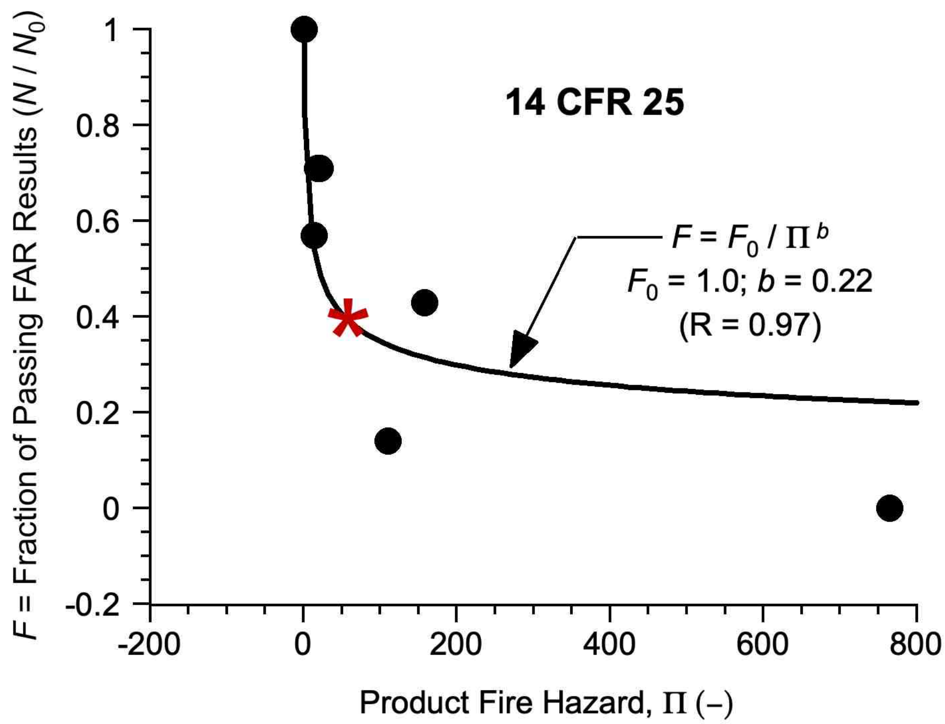

Figure 10. Fire resistance of aviation products, FR Π N/N0 versus Π

The coefficients of the phlogistic response function in the legend of Figure 11 indicate that a material at the fire hazard threshold of Figure 10, Π* = 67, has a 61% chance of flashover in a post-crash fire, while the chance of cabin flashover for products meeting Quintiere's ISO 9705 criterion, Π = 2.78, is only 10%. The variance in p is $\sigma_p^2 = p(1-p)$ (Lyon & Safronava, A Probabilistic Analysis of Pass/Fail Fire Tests, Final Report DOT/FAA/TC-12/13, 2013), so the difference between $p(\Pi^*)$ and $p(\Pi_0)$ is statistically indistinguishable. These results suggest a performance-based (rather than a threat-based) classification scheme for fire safety of aircraft cabin materials, as indicated in the legend of Figure 11.

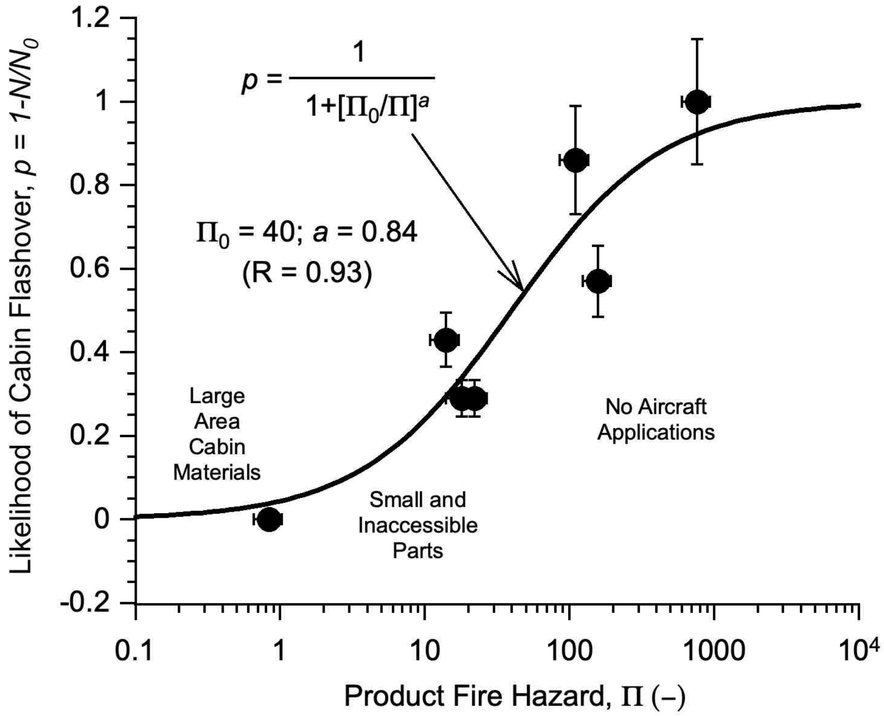

Figure 11. Probabilistic Analysis of the Data in Figure 10 for Full-Scale Fire Performance of Aircraft Cabin Materials.

4.5 International fire safety classification of building products

Table 6 compares classification schemes for the fire hazard of construction products and the test method used for rating the fire safety of these products by the United States according to the IBC; the European Union (EU) classification according to EN 13501-1; the Australian (AU) classification according to the Building Code of Australia (BCA); and the Japanese (JP) classification according to the Building Standards Law (BSL) (Janssens, Carpenter, Huczek, Mehrafza, & Sauceda, 2006). The first column of Table 6 is a numerical rating of the international classifications in descending order from most severe ($F = 4$) to least severe ($F = 1$).

Table 6. International fire safety classification of construction products

Fire Safety Rating, F	Country/Region			
	US	**EU**	**AU**	**JP**
4	A	A2/B	Group d	Non-Combustible
3	B	C	Group c	Quasi-Combustible
2	C	D	Group b	Flame Retardant
1	Unclassified	E/F	Group a	Unclassified
Test Method	**ASTM E84**	**EN 13823**	**ISO 9705**	**ISO 5660-1**
Regulation	**IBC**	**EN 13501-1**	**BCA**	**BSL**

Table 7 lists the fire hazard Π of each product in Table 2 along with a numerical fire safety rating for each product in each country/region from Table 6 and the average international rating, $\bar{F}$. Figure 12 is a plot of the average international fire safety rating $\bar{F}$ *versus* Π for the products in Table 7.

Table 7. International fire safety classification of Table 6 ranked by Π for products in Table 2

Product	Π (–)	International Fire Safety Rating				$\bar{F}$
		US	**EU**	**AU**	**JP**	
Type X Gypsum Board	1	4	4	4	4	4
Paper Wall Covering	1	–	–	–	–	–
Vinyl Wall Covering	11	3	3	3	4	3.25
Textile Wall Covering	29	–	–	–	–	–
FRT Douglas Fir Plywood	117	4	3	3	1	2.75
Douglas Fir Plywood	199	2	2	2	1	1.75
Glass Fiber Reinforced Plastic	246	2	1	2	1	1.50
Oriented Strand Board 2	293	2	2	2	1	1.75
White Oak Planks	313	2	2	2	1	1.75
Oriented Strand Board 1	366	2	2	2	1	1.75
White Pine Planks	397	2	2	2	1	1.75
Polyisocyanurate Foam	1084	2	1	1	1	1.25
Test Method	**ASTM E1354**	**ASTM E84**	**EN 13823**	**ISO 9705**	**ASTM E1354**	
National/Regional Regulation		**IBC**	**EN 13501-1**	**BCA**	**BSL**	

The solid line in Figure 12 is a fit of Equation 12 to the data points with nonlinear least squares regression coefficients, F_0 = 4.19, b = 0.15 (R = 0.94). Figure 11 shows that Π provides a consistent ranking of product fire hazard across international standards, with a fire safety threshold, Π* = 87, F^* = 2.14 for Π_{max} = 1084, $\bar{F}_{max}$= 4 of Table 7. The international fire safety threshold is comparable to the thresholds for a wider range of products in a subset of these regulatory fire tests, Π* = 68 ± 5 (Figure 7, Figure 9, and Figure 10).

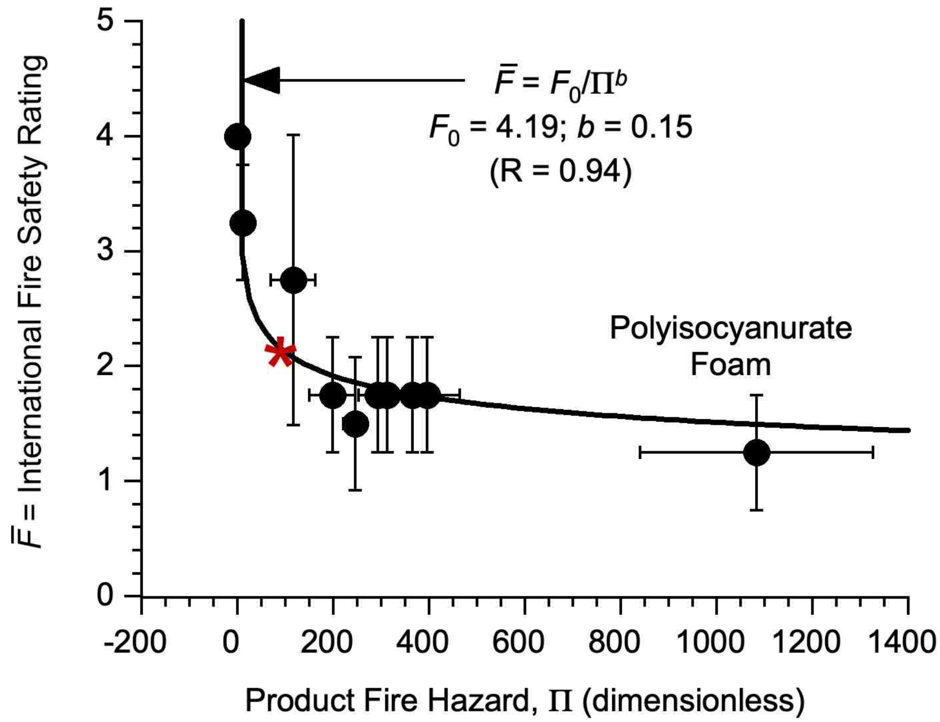

Figure 12. Average international fire safety rating $\bar{F}$ versus Π for the products in Table 7

5 Summary and conclusions

The fire hazard of a product, Π of Equations 5-7, is a dimensionless group of reaction-to-fire parameters that can be computed from derived fire properties (HRP, TRP, $\dot{Q}''_{cr}$) or directly from fire test parameters ($\dot{q}''_{ext}, \dot{Q}''_{max}, t_{ign}, Q''_{total}$) measured in one or more standard cone calorimeter experiments:

$$\Pi = \frac{HRP\ \dot{q}''_{ext}}{TRP^2/Q''_{total}} = \frac{THR\ \dot{Q}''_{burn}}{TRP^2/Q''_{total}} = \frac{\dot{Q}''_{max}/t_{ign}}{\dot{q}''^{\,2}_{ext}/Q''_{total}}$$

These forms of Π are equivalent to within the uncertainty of the calculation from component properties (Figure 4, Figure 5, and Figure 6) and they capture the trend of fire test results for forced flaming combustion (Figure 7, Figure 8, Figure 9, Figure 10, Figure 11, and Figure 12) in the derived relationship (Equation 12):

$$F = \frac{F_0}{\Pi^b}$$

The product fire hazard has a threshold in fire tests of forced burning above which rapid fire growth is observed:

$$\Pi^* = \left[\frac{b\Pi_{max}}{F_{max}/F_0}\right]^{\frac{1}{1+b}}$$

The product burning resistance at the fire safety threshold F^* is proportional to Π^* for a particular fire test (b, $F_{\max}$) and selection of products ($\Pi_{\max}$) and is obtained from Equation 12 and Equation 14 as

$$F^* = \frac{F_0}{\Pi^*} = \frac{F_{max}/\Pi_{max}}{b} \cdot \Pi^* = C(b) \cdot \Pi^*$$

Table 8 is a performance-based classification scheme for products across international regulatory codes, independent of the definition of combustibility, the fire test/scenario and the sample dimensions that is suggested by the data in Tables 1-7, Figures 4-12, and supporting analyses.

Table 8. Performance-based classification scheme

Classification	**$LOG_{10}\ \Pi$**
A	≤ 0
B	0-1
C	1-2
D	2-3
None	≥ 3

6 References

ASTM International. (2023). ASTM E1354-23 Standard Test Method for Heat and Visible Smoke Release Rates for Materials and Products Using an Oxygen Consumption Calorimeter. West Conshohocken, PA: ASTM International.

ASTM International. (2023). Standard Test Method for Determining Surface Burning Characteristics of Building Materials. *UL 723 Underwriters Laboratories (2023) and ASTM E84*. West Conshohocken, PA.

Babrauskas, V. (2017). Engineering Variables to Replace the Concept of 'Noncombustibility. *Fire Technology, 53*, 353-373.

Cleary, T. G., & Quintiere, J. G. (1991). A Framework for Utilizing Fire Property Tests. *Proceedings of the Third International Symposium on Fire Safety Science* (pp. 647-656). New York: Elsevier Applied Science.

Federal Aviation Administration. (2000). Aircraft Materials Fire Test Handbook. In A. Horner (Ed.), *Aircraft Materials Fire Test Handbook.*

Federal Aviation Administration, D. o. (2004). Title 14 Aeronautics and Space, Part 25 Airworthiness Standards: Transport Category Airplanes, Section 853 Compartment Interiors. In U. Gov, *Code of Federal Regulations* (p. Chapter 1). Washington D.C., Washington D.C.: US Government Printing Office.

Hill, R. G., Brown, L. J., Speitel, L., Johnson, G. R., & Sarkos, C. (1984). *Aircraft Seat Fire Blocking Layers; Effectiveness and Benefits Under Various Fire Scenarios.* Final Report DOT/FAA/CT-83/43.

Hill, R. G., Eklund, T. I., & Sarkos, C. P. (1985). *Aircraft Interior Panel Test Criteria Derived from Full-Scale Fire Tests.* Final Report DOT/FAA/CT-85/23.

International Organization for Standardization. (2002). ISO 5660-1: Reaction-to-Fire Tests-Heat Release, Smoke Production and Mass Loss Rate-Part 1:(Cone Calorimeter Method). Geneva, Switzerland: International Organization for Standardization.

International Organization for Standardization. (2016). Full Scale Room Test for Surface Products. *ISO 9705-1*. Geneva, Switzerland.

Janssens, M., Carpenter, K., Huczek, J., Mehrafza, M., & Sauceda, A. (2006). Performance of Construction Products in Reaction-to-Fire Tests. *17th Annual BCC Conference on Flame Retardancy.* Stamford, CT.

Janssens, M., Carpenter, K., Huczek, J., Mehrafza, M., & Sauceda, A. (n.d.). Private communication.

Lyon RE, C. S. (2021). Fire Properties of Combustible Materials from Unsteady Burning. *Fire Safety Journal, 120, 103054*.

Lyon, R. E. (2024). Measuring the Fire Growth Potential of Combustible Solids Using a Cone Calorimeter. *Journal of Fire Sciences, 42(6)*, 487-513.

Lyon, R. E., & Quintiere, J. G. (2007). Criteria for Piloted Ignition of Combustible Solids. *Combustion and Flame, 151*, 551-559.

Lyon, R. E., & Safronava, N. (2013). *A Probabilistic Analysis of Pass/Fail Fire Tests, Final Report DOT/FAA/TC-12/13.* Federal Aviation Administration.

Ostman, B., & Janssens, M. (2022). Reaction-to-Fire Performance, in Fire Safe Use of Wood in Buildings. CRC Press.

Ostman, B., & Tsantaridis, L. D. (1994). Correlation Between Cone Calorimeter Data and Time to Flashover in the Room Fire Test. *Fire and Materials, 18*, 205-209.

Ostman, B., & Tsantaridis, L. D. (1995). Heat Release and Classification of Fire-Retardant Wood Products. *Fire and Materials, 19*, 253-258.

Quintiere, D., & Lian. (2009). Inherent Flammability Parameters—Room Corner Test Application. *Fire and Materials: An International Journal, 33(8)*, 377-393.

Rasbash, D. J. (1976). Theory in the Evaluation of Fire Properties of Combustible Materials. *Proc. 5th International Fire Protection Seminar*, (pp. 113-130). Karlsruhe, Germany.

Sadaoui A, D. C. (2024). The Evolution of Reaction to Fire Classification of Materials: A Case Study of Canada. *Fire and Materials 48*, 737-751 .

Safronava N, L. R. (August 2022). *Microscale Flammability Criterion for Constituents of Aircraft Cabin Materials.* Final Report DOT/FAA/TC-22/22.

Tewarson, A. (1994). Flammability Parameters of Materials: Ignition, Combustion, and Fire Propagation. *Journal of Fire Sciences, 12*, 329-356.

Tewarson, A. (1996). Flammability. In E. Mark JE, *Physical Properties of Polymers Handbook* (p. Chapter 42). New York: AIP Press.